CONDITIONS OF PHYSICAL SOLVABILITY OF TWO- AND THREE-ZONE LINEAR STORAGE MODELS*

Š. Dvořáková, J. Zeman

Czech University of Life Sciences Prague, Faculty of Engineering, Prague, Czech Republic

The article deals with finding several interesting relationships, which arise by using very reasonable assumptions from using two- and three-zone models for the properties of matrix elements, which characterize various physical parameters of the catchment area. These relationships have the character of both equality and inequality and are the result of physical solvability of emergent system of linear equations, particularly of the requirements of reality and positivity of eigenvalues of the matrix.

hydrological watershed model; linear storage model; condition of solution; hydrological catchment parameters; depletion time; two- and three-zone linear model

INTRODUCTION

For a description of flow dynamics of small catchments, the linear storage models are successfully used especially for the dry periods. The simplified variant of such models is used for example for the comparison of two catchments in northern Tanzania (Mul et al., 2007), one covering less than 1 km^2, and the other approximately 25 km^2. At a larger scale, the influence of this hydrological process is no longer visible. Another interesting comparison between two models was given by Winsemius et al. (2006).

The impact of plants and their respiration on groundwater runoff was dealt with by Troxell (1936) and Balek (2006). Furthermore, the effect of actual evapotranspiration when depleted by riparian vegetation should be considered on small catchments as a diurnal (day-night) process lasting from sunrise to sunset. In this study, two catchments were observed (Teply brook and Starosuchdolsky brook) representing a specific hydrologic phenomenon of diurnal discharges fluctuation which can reduce almost one third of daily runoff on very small catchments during hot summer rainless periods. Difference in day and night behaviour of drainage from separate zones was investigated by Burt (1979).

In previous papers (Dvořáková, Zeman, 2010a, b) the sequential assembling of a linear storage model was discussed. This model was applied to the specific catchments of Teply brook (1.56 km^2) and Starosuchdolsky brook (2.95 km^2). During the solution of backward task, i.e. looking for parameters of the catchment (volume of the individual zones, porosity) from a known discharge, it is useful to know the limits of the values of searched coefficients. Finding some of these limits is the subject of the present paper.

The linear retention model was developed primarily to describe the total channel flow of a small watershed in rainless period. This model is designed as linear and the easiest possible for the description of all the significant effects on the runoff in a dry season. It is based on the idea of three interconnected tanks of water. Each of these tanks represents a specific subsurface layer with a total volume of water and time-dependent volume of available water, which participates in the runoff process. Each of these layers contributes to the total channel flow. The evapotranspiration is approximated by the sinus harmonic function.

The LSM model more tightly fits the typical measured data, which are displayed in Discussion. It is the Starosuchdolsky Brook discharge in the rainless period of June 22–30, 2012.

MATERIAL AND METHODS

For the description of the surveyed catchments (Teply and Starosuchdolsky brooks) in dry summer days the linear approximation provides a sufficient precision. Therefore two- and three-zone linear runoff

* Supported by the Ministry of Agriculture of the Czech Republic, Project No. QJ1220033, and by the Technology Agency of the Czech Republic, Project No. TA02020402.

Table 1. Characteristics of the Starosuchdolsky brook catchment

Catchment area/basin (km^2)	2.946
Maximum catchment elevation (m a.s.l.)	335
Minimum catchment elevation (outlet) (m a.s.l.)	211
Elevation of brook source (m a.s.l.)	230
Length of thalweg (km)	3.7
Length of brook (km)	0.58
Length of catchment divide (km)	9.1
Average slope of brook (%)	5.4
Shape of catchment	0.2

models have been developed. The effect of evapotranspiration was approximated by the first member of the Fourier series.

Own data on the Starosuchdolsky Brook catchment were used for the example of the two-zone model. Characteristics of the catchment are listed in Table 1 (coordinates of the outlet 50.1465´N, 14.3831´E).

RESULTS

In the previous work, a basin model (Fig. 1) consisting of the upper subsurface, lower subsurface, and groundwater reservoir was developed including flow coefficients:

$$\begin{aligned}
&i = i_{11} + i_{22} + i_{33}\\
&i_{11} = a_{11} \cdot h_1\\
&i_{22} = a_{22} \cdot h_2\\
&i_{33} = a_{33} \cdot h_3\\
&i_{21} = a_{21} \cdot (h_2 - h_1)\\
&i_{32} = a_{32} \cdot (h_3 - h_2)\\
&\frac{dh_1}{dt} = \frac{1}{V_1}(i_{21} - i_{11}) = \frac{1}{V_1}(a_{21} \cdot (h_2 - h_1) - a_{11} \cdot h_1) =\\
&\quad = \frac{1}{V_1}(h_1(-a_{21} - a_{11}) + h_2 \cdot a_{21})\\
&\frac{dh_2}{dt} = \frac{1}{V_2}(i_{32} - i_{21} - i_{22}) =\\
&\quad = \frac{1}{V_2}(a_{32} \cdot (h_3 - h_2) - a_{21} \cdot (h_2 - h_1) - a_{22} \cdot h_2) =\\
&\quad = \frac{1}{V_2}(h_1 \cdot a_{21} + h_2(-a_{32} - a_{21} - a_{22}) + h_3 \cdot a_{32})\\
&\frac{dh_3}{dt} = \frac{1}{V_3}(-i_{33} - i_{32}) = \frac{1}{V_3}(-a_{32} \cdot (h_3 - h_2) - a_{33} \cdot h_3) =\\
&\quad = \frac{1}{V_3}(h_3(-a_{32} - a_{33}) + h_2 \cdot a_{32})
\end{aligned} \tag{1}$$

This model is conceptually similar to the models used in the literature (e.g. Fenicia et al., 2006; Mul et al., 2007). It mathematically corresponds to the solution of linear systems of differential equations with the non-zero right side (1). Here, the elements of the matrix **B** are given by the catchment hydrological parameters (2).

$$\mathbf{B} = \begin{pmatrix} \frac{-a_{21} - a_{11}}{V_1} & \frac{a_{21}}{V_1} & 0\\ \frac{a_{21}}{V_2} & \frac{-(a_{32} + a_{21} + a_{22})}{V_2} & \frac{a_{32}}{V_2}\\ 0 & \frac{a_{32}}{V_3} & \frac{-(a_{32} + a_{33})}{V_3} \end{pmatrix} \tag{2}$$

where:
a_{11} = groundwater runoff into the flow
a_{22} = runoff from the lower subsurface layer to the flow
a_{33} = runoff from the upper subsurface layer to the flow
a_{21} = runoff from lower subsurface reservoir to groundwater reservoir
a_{31} = equals 0, because the groundwater does not flow directly to the upper subsurface layer
a_{32} = runoff from upper subsurface reservoir to lower subsurface reservoir
h_1 = relative groundwater level (-)
h_2 = relative lower subsurface water level (-)
h_3 = relative upper subsurface water level (-)
V_1 = relative volume (porosity) of groundwater reservoir (-)
V_2 = relative volume (capacity) of lower subsurface water reservoir (-)
V_3 = relative volume (capacity) of upper subsurface water reservoir (-)
ξ = evapotranspiration

In the case of extreme water level, when the upper subsurface zone is exhausted by drought, the model can be simplified to only two-zones model, whose parameters are represented by the matrix **B**´ (size 2 × 2). This model is represented by eq. (3) (Fig. 3):

$$\mathbf{B} \cdot \vec{h} - \frac{d\vec{h}}{dt} = \vec{\xi} \tag{3}$$

where:

$$\vec{\xi} = \begin{pmatrix} 0\\ 0\\ K(\sin \omega t + 1) \end{pmatrix}$$

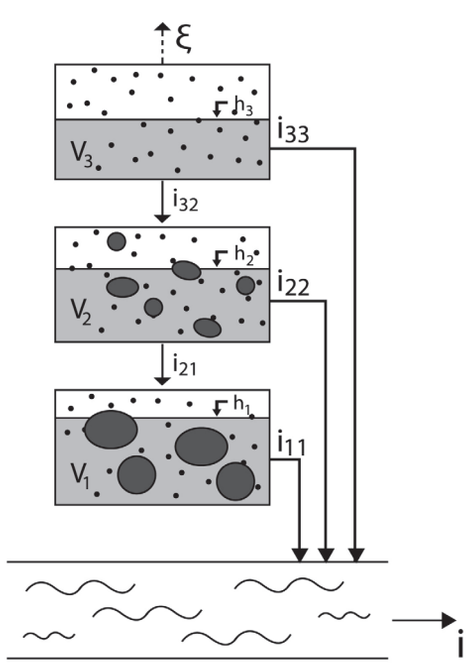

Fig. 1. Scheme of the LSM model

We solve this equation by finding eigenvalues λ and eigenvectors of matrix **B**. We find, therefore, for which λ is the determinant of the matrix **B**-λE equal to zero (4).

$$\det(\mathbf{B}-\lambda\mathbf{E}) = \begin{vmatrix} \frac{-a_{21}-a_{11}}{V_1}-\lambda & \frac{a_{21}}{V_1} & 0 \\ \frac{a_{21}}{V_2} & \frac{-(a_{32}+a_{21}+a_{22})}{V_2}-\lambda & \frac{a_{32}}{V_2} \\ 0 & \frac{a_{32}}{V_3} & \frac{-(a_{32}+a_{33})}{V_3}-\lambda \end{vmatrix} = 0 \quad (4)$$

Using this procedure we find the solution of eq. (3) in the form of eq. (5), whose roots are λ_1, λ_2, λ_3.

The basis for the claim in this paper is the assumption based on the experience that in the realistic catchment there are not oscillations, where own frequency of periodical changes of the water level is given by watershed parameters. On the contrary, all observations suggest that the basin is drained according to the curve which is well described as a sum of exponentials. The next and of course sensible and yet more general assumption is that we expect the negative exponential coefficients, because in the opposite case there would be an increase of drained water over all limits. The expected shape of the flow of the depleted catchment has the following form:

$$\overrightarrow{h(t)} = e^{\lambda_1 t}\overrightarrow{k} + e^{\lambda_2 t}\overrightarrow{l} + e^{\lambda_3 t}\overrightarrow{m} + \overrightarrow{n} \quad (5)$$

alternatively $\overrightarrow{h(t)} = e^{-\frac{-1}{\tau_1}t}\overrightarrow{k} + e^{-\frac{-1}{\tau_2}t}\overrightarrow{l} + e^{-\frac{-1}{\tau_3}t}\overrightarrow{m} + \overrightarrow{n}$

where $\tau_1 = \frac{1}{|\lambda_1|}$ $\tau_2 = \frac{1}{|\lambda_2|}$ $\tau_3 = \frac{1}{|\lambda_3|}$.

Here the coefficients τ_1, τ_2, τ_3 are real and greater than zero, and they represent the depletion times of the individual zones. This solution of eq. (1) corresponds well with the reality, at least in some cases, as has been shown in the paper by D v o ř á k o v á et a1. (2012). The requirements for reasonable physical solution of eq. (3) tell us that (1) the coefficients λ_1, λ_2, λ_3 are real and (2) the coefficients λ_1, λ_2, λ_3, which are eigenvalues of matrix **B**, are negative.

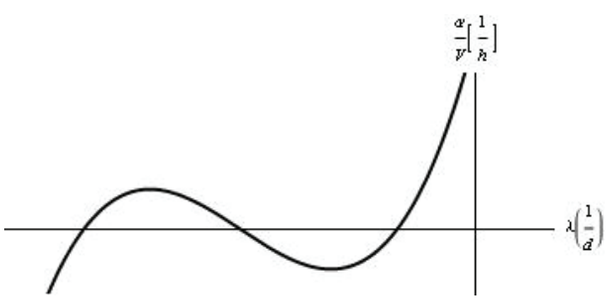

Fig. 2. A typical characteristic polynomial of the three-zone catchment

Characteristic polynomial for this three-zone model can be seen in Fig. 2.

Assumptions 1 and 2, in their mathematical result, mean that the eigenvalues of the matrix **B** are all negative. This simple result leads to the formulation of several relationships between coefficients of the catchment in the matrix **B**. Eigenvalues λ_1, λ_2, λ_3 are the roots of the characteristic polynomial of the 3rd order of the matrix **B** and this polynomial has the form of eq. (6):

$$A\lambda^3 + B\lambda^2 + C\lambda + D = 0 \quad (6)$$

From assumptions 1 and 2, several equations and inequalities for the coefficients of this polynomial follow.

Namely, the coefficients A and D have the same sign in accordance with Cardanós formulas. Also, from Fig. 2 it is clear that local extremes of such a polynomial of the 3rd order, which satisfy the requirements 1 and 2, lie between λ_1 and λ_3, which are negative and real. Further it can be said that the characteristic polynomial function values in these extreme points have opposite signs. The values of λ_1^*, λ_2^* extremes we obtain by solving eq. (7):

$$3At^2 + 2Bt + C = 0 \quad (7)$$

Real discriminant of the equation is greater than 0, i.e.

$$4B^2 - 12AC > 0 \quad (8)$$

The graph similar to the polynomial (7) can be seen in Fig. 4 from which it is clear again that the extreme of this parabola for λ is less than zero. This is actually the inflection point of the characteristic eq. (4) and we have –B/3A < 0, i.e. the coefficients A and B have the same signs, and at the same time we have

$$4B^2 - 12AC < (2B)^2 \quad (9)$$

The coefficients A–D in eq. (6) detailed for the **B** matrix coefficients are equal to eq. (10):

$$\begin{aligned} A &= V_1V_2V_3 \\ B &= V_1V_2(a_{32}+a_{33}) + V_1V_3(a_{32}+a_{21}+a_{22}) + V_2V_3(a_{21}+a_{11}) \\ C &= V_1(a_{32}+a_{21}+a_{22})(a_{32}+a_{33}) + V_2(a_{21}+a_{11})(a_{32}+a_{33}) + \\ &\quad + V_3(a_{21}+a_{11})(a_{32}+a_{21}+a_{22}) - V_3a_{21}^2 - V_1a_{32}^2 \\ D &= (a_{21}+a_{11})(a_{32}+a_{21}+a_{22})(a_{32}+a_{33}) - \\ &\quad - a_{21}^2(a_{32}+a_{33}) - a_{32}^2(a_{21}+a_{11}) \end{aligned} \quad (10)$$

After substituting these values into inequalities (8), (9) found above, we find more detailed inequalities in the form (11), (12)

$$\begin{aligned} &4\left[V_1V_2(a_{32}+a_{33}) + V_1V_3(a_{32}+a_{21}+a_{22}) + V_2V_3(a_{21}+a_{11})\right]^2 - \\ &-12V_1V_2V_3\left[V_1(a_{32}+a_{21}+a_{22})(a_{32}+a_{33}) + \right. \\ &\left. + V_2(a_{21}+a_{11})(a_{32}+a_{33}) + V_3(a_{21}+a_{11})(a_{32}+a_{21}+a_{22}) - \right. \\ &\left. - V_3a_{21}^2 - V_1a_{32}^2\right] > 0 \end{aligned} \quad (11)$$

$$4\left[V_1V_2(a_{32}+a_{33})+V_1V_3(a_{32}+a_{21}+a_{22})+V_2V_3(a_{21}+a_{11})\right]^2$$
$$-12V_1V_2V_3\left[V_1(a_{32}+a_{21}+a_{22})(a_{32}+a_{33})+V_2(a_{21}+a_{11})(a_{32}+a_{33})+\right.$$
$$\left.+V_3(a_{21}+a_{11})(a_{32}+a_{21}+a_{22})-V_3a_{21}^2-V_1a_{32}^2\right]<$$
$$<(2V_1V_2(a_{32}+a_{33})+V_1V_3(a_{32}+a_{21}+a_{22})+V_2V_3(a_{21}+a_{11}))^2 \quad (12)$$

Now let us have a look at the inequalities arising from the conditions 1 and 2 for two-zone LSM, which is presented in Fig. 3 and described by eq. (13).

$$\begin{aligned} i &= i_{11}+i_{22} \\ i_{11} &= a_{11}\cdot h_1 \\ i_{22} &= a_{22}\cdot h_2 \\ i_{21} &= a_{21}\cdot(h_2-h_1) \\ \frac{dh_1}{dt} &= \frac{1}{V_1}(i_{21}-i_{11}) = \frac{1}{V_1}(a_{21}\cdot(h_2-h_1)-a_{11}\cdot h_1) = \\ &= \frac{1}{V_1}(h_1(-a_{21}-a_{11})+h_2\cdot a_{21}) \\ \frac{dh_2}{dt} &= \frac{1}{V_2}(-i_{21}-i_{22}) = \frac{1}{V_2}(-a_{21}\cdot(h_2-h_1)-a_{22}\cdot h_2) = \\ &= \frac{1}{V_2}(h_1\cdot a_{21}+h_2(-a_{21}-a_{22})) \end{aligned} \quad (13)$$

i.e. we get the matrix **B´** in the form

$$\mathbf{B}' = \begin{pmatrix} \frac{-a_{21}-a_{11}}{V_1} & \frac{a_{21}}{V_1} \\ \frac{a_{21}}{V_2} & \frac{-a_{21}-a_{22}}{V_2} \end{pmatrix} \quad (14)$$

and we solve the equation which is similar to eq. (3):

$$\mathbf{B}'\cdot\overrightarrow{h}-\frac{d\overrightarrow{h}}{dt}=\overrightarrow{\xi'} \quad (15)$$

where:

$$\overrightarrow{\xi'} = \begin{pmatrix} 0 \\ 0 \\ K'(\sin\omega t+1) \end{pmatrix}$$

Eigenvalues of matrix **B´** we count with determinant of matrix **B´**, thus

$$\det(\mathbf{B}'-\lambda'\mathbf{E}) = \begin{vmatrix} \frac{-a_{21}-a_{11}}{V_1}-\lambda' & \frac{a_{21}}{V_1} \\ \frac{a_{21}}{V_2} & \frac{-a_{21}-a_{22}}{V_2}-\lambda' \end{vmatrix} = 0 \quad (16)$$

gives (after writing out the **B´** matrix coefficients) the values

$$\lambda'_1 = \frac{1}{2V_1V_2}(-a_{21}V_1-a_{22}V_1-a_{11}V_2-a_{21}V_2- \quad (17)$$
$$-\sqrt{-4(a_{11}a_{21}+a_{11}a_{22}+a_{21}a_{22})V_1V_2+(a_{21}V_1+a_{22}V_1+a_{11}V_2+a_{21}V_2)}$$

A typical process of the characteristic polynomial arising from eq. (16) can be seen in Fig. 4 and it is described by eq. (18). To this polynomial we put similar conditions as in the case of three-zone LSM.

$$A'\lambda'^2+B'\lambda'+C'=0 \quad (18)$$

From the first condition $\lambda'_1,\lambda'_2\in R$, i.e. the discriminant is

$$B'^2-4A'C'>0 \quad (19)$$

From the second condition $\lambda'_1,\lambda'_2<0$, we get

$$B'^2-4A'C'<(2B')^2 \quad (20)$$

From the necessity, that the extreme time coordinate of the parabola in Fig. 4 was also negative, from the derivative of the function (18) the condition –B´/2A´ < 0 (for A´ not equal to zero) is obtained, hence A´and B´ have the same signs.

After substitution we have relationships for the hydrological parameters:

$$\begin{aligned} A' &= V_1V_2 \\ B' &= V_1(a_{21}+a_{22})+V_2(a_{21}+a_{11}) \\ C' &= a_{11}a_{21}+a_{21}a_{22}+a_{11}a_{22} \end{aligned} \quad (21)$$

And by substitutions in the relations (19), (20), for the coefficients of two-zone LSM model we get the conditions (22), (23):

$$(V_1(a_{21}+a_{22})+V_2(a_{21}+a_{11}))^2- \quad (22)$$
$$-4V_1V_2(a_{11}a_{21}+a_{21}a_{22}+a_{11}a_{22})>0$$

$$(V_1(a_{21}+a_{22})+V_2(a_{21}+a_{11}))^2- \quad (23)$$
$$-4V_1V_2(a_{11}a_{21}+a_{21}a_{22}+a_{11}a_{22})>$$
$$>(2(V_1(a_{21}+a_{22})+V_2(a_{21}+a_{11})))^2$$

DISCUSSION

We look for nine parameters of a long-time series in the three-zone model, which typically contain hun-

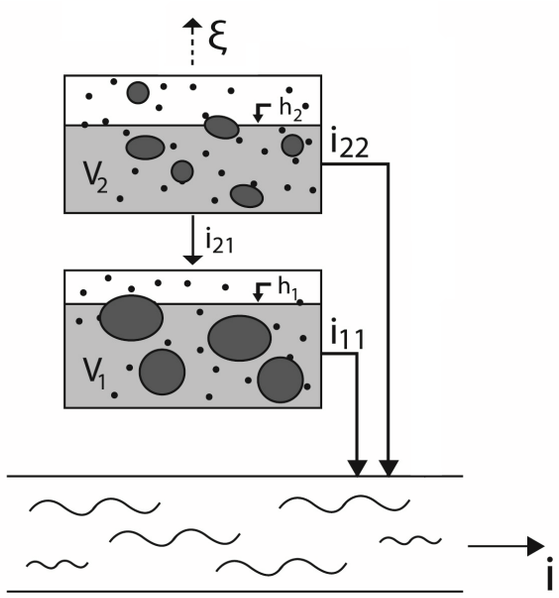

Fig. 3. Scheme of two-zone LSM model

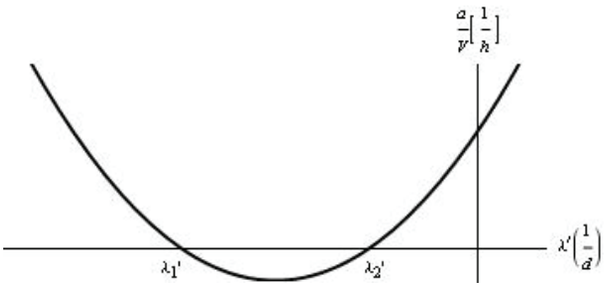

Fig. 4. A typical characteristic polynomial of two-zone catchment

dreds of thousands of values what is the task on the boundary of computer possibilities.

While the direct calculation of the model when we look for the solution from the known elements of the matrix **B´** is easy, an inverse finding of matrix **B´** elements which give the solution in accordance with the LSM method as close as possible to the hundreds of thousands of measured values is a difficult task. In addition, the searched optimum should be, if possible, global and must meet the conditions of positivity of matrix elements and of the water level of each zone.

This problem also explains why it is not efficient to solve more complicated models, e.g. four-zone, because the solution of backward task for such a problem is not numerically realistic at present. To a worse situation we get when we try to use non-linear models. From this point of view it seems that currently for the backward task the linear three-zone model is piecewise having the same restrictions for parameter values as are found above.

The example of the application of two-zone LSM model on real data is given in Fig. 5 where the flow of the Starosuchdolsky Brook during the rainless period June 22–30, 2013 is displayed. From the model we obtain the parameters of the catchment area shown in Table 2.

Table 2. Parameters of the catchment area

	Correct parameter	Incorrect parameter
V_1 (m^3)	7.17	7.17
V_2 (m^3)	599.24	599.24
a_{11} ($l.s^{-1}$)	2.086	2.179
a_{21} ($l.s^{-1}$)	18.218	21.243
a_{22} ($l.s^{-1}$)	0.315	0.791
$h_1(0)$ (%)	13.982	15.723
$h_2(0)$ (%)	12.283	20.066

V_1 = relative volume (porosity) of groundwater reservoir, V_2 = relative volume (capacity) of lower subsurface water reservoir, a_{11} = groundwater runoff into the flow, a_{21} = runoff from lower subsurface reservoir to groundwater reservoir, a_{22} = runoff from the lower subsurface layer to the flow, h_1 = relative groundwater level, h_2 = relative lower subsurface water level

The accuracy of the implemented model calibration, i.e. consistency between the measured flow values and the calculated flow values, is expressed by two statistical criteria, the determination coefficient, called the Nash-Sutcliffe efficiency coefficient (Nash, Sutcliffe, 1970), and the variation coefficient:

$$CD = 1 - \frac{\sum (Q_m - Q_v)^2}{\sum (Q_m - \overline{Q}_m)^2} \quad \text{and} \quad CV = \frac{\sqrt{\frac{\sum (Q_m - Q_v)^2}{n}}}{\overline{Q_m}}$$

where:

Q_m = measured discharges ($l.s^{-1}$)

Q_v = calculated discharges ($l.s^{-1}$)

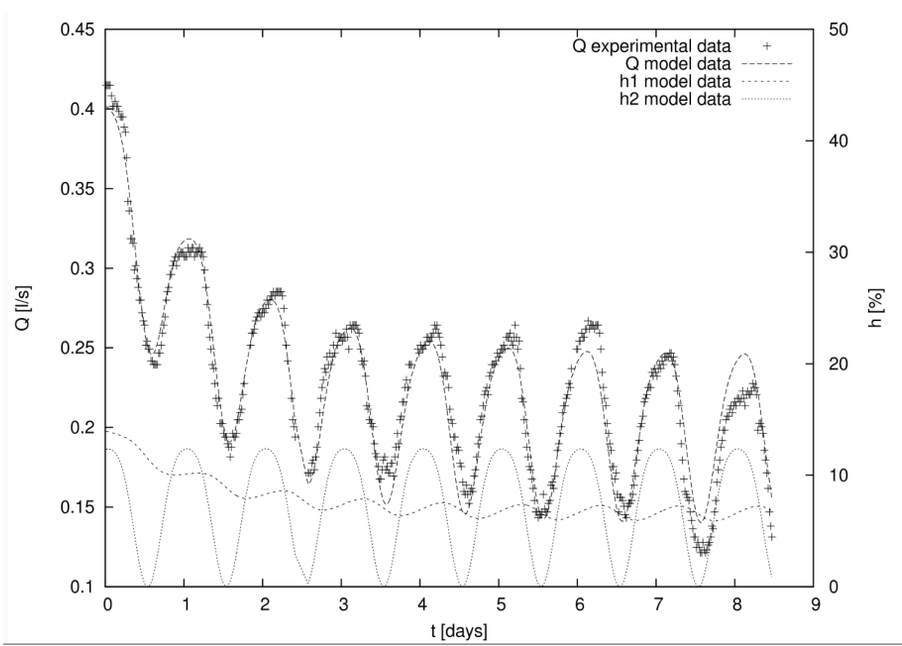

Fig. 5. Example of comparison of model courses with measured data

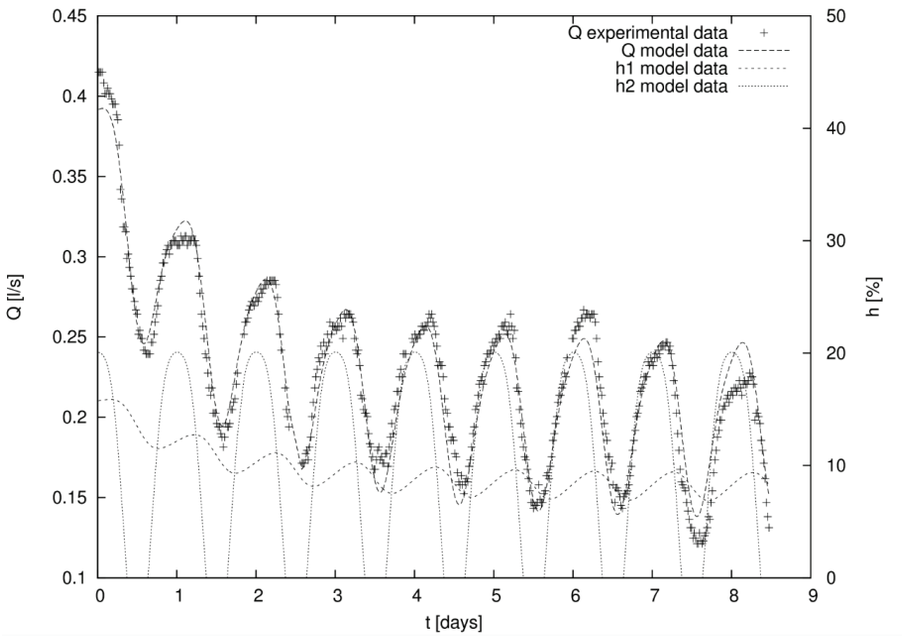

Fig. 6. Example of the incorrect solution of matrix **B´**

$\overline{Q_m}$ = mean value of measured discharges (l.s^{-1})

n = number of measured values

The coefficient of determination CD in best fit conditions equals to 1.0; on the other hand, the coefficient of variation CV in ideal conditions equals to 0.0 (C h o w et al., 1988).

In our case, the mentioned coefficients are CD = 0.76 and CV = 0.14.

In search of the best elements of the matrix **B´** the solution is often incorrect (see Fig. 6). The correct solution can be found only by the application of conditions (19) and (20) (Fig. 5). As can be seen, the solutions differ from each other mainly by non-negativity of all values $h_2(t)$.

CONCLUSION

In this work, we managed to build relational terms of coefficients in the two- and three-zone LSM model. The usability of these terms is particularly evident in the efforts to resolve inverse tasks when by using the fitting we look for the coefficients for specific basins at specified flow rates. In these simulations, it is necessary to supervise that values of searched parameters which are changed by computing algorithm do not vary from the presented relations and therefore the evaluation does not end by breakdown or takes too long time.

Another aspect of the relation can be found in the search for physical or hydrological interpretations. They put to relation properties of water with the porosity of different zones that actually occur in nature. It appears that the relations between these variables are not random, but in all known cases they fulfil the relations that have already been described.

REFERENCES

Balek J (2006): Small basins as a continuous source of information. Journal of Hydrology and Hydromechanics, 54, 96. (in Czech)

Burt TP (1979): Diurnal variations in stream discharge and throughflow during a period of low flow. Journal of Hydrology, 41, 291–301. doi: 10.1016/0022-1694(79)90067-2.

Chow VT, Maidment DR, Mays LW (1988): Applied Hydrology. Ed. McGraw-Hill, New York, USA.

Dvořáková Š, Zeman J (2010a): Analysis of fluctuation in the stream water level during the dry season in forested areas. Scientia Agriculturae Bohemica, 41, 218–224.

Dvořáková Š, Zeman J (2010b): Differential model of summer circulation. Trends in Agricultural Engineering, 4, 142-145.

Dvořáková Š, Kovář P, Zeman J (2012): Implementation of conceptual linear storage model of runoff with diurnal fluctuation in rainless periods. Journal of Hydrology and Hydromechanics, 60, 4, 217–226. doi: 10.2478/v10098-012-0019-y.

Fenicia F, Savenije HHG, Matgen P, Pfister L (2006): Is the groundwater reservoir linear? Learning from data in hydrological modelling. Hydrology and Earth System Science, 10, 139–150.

Mul ML, Savenije HHG, Uhlenbrook S (2007): Base flow fluctuations from a forested and a cultivated hill slope in

northern Tanzania. In: Proc. 8th WATERNET/WARFSA/GWP-SA Symposium, Lusaka, Zambia, xx–xx. (CD-Rom)

Nash JE, Sutcliffe JV (1970): River flow forecasting through conceptual models. Part I – A discussion of principles. Journal of Hydrology, 10, 282–290. doi: 10.1016/0022-1694(70)90255-6.

Troxell HC (1936): The diurnal fluctuation in the groundwater and flow of the Santa Ana River and its meaning. Transaction of American Geophysical Union, 17, 496–504.

Winsemius HC, Savenije HHG, Gerrits AMJ, Zapreeva EA, Kless R (2006): Comparison of two model approaches in the Zambezi river basin with regard to model reliability and identifiability. Hydrology and Earth System Science, 10, 339–352. doi: 10.5194/hess-10-339-2006.

Received for publication on January 29, 2013
Accepted for publication on Novemberr 15, 2013

Corresponding Author:

Ing. Šárka D v o ř á k o v á , Ph.D., Czech University of Life Sciences Prague, Faculty of Engineering, Department of Mathematics, Kamýcká 129, 165 21 Prague 6-Suchdol, Czech Republic, phone: +420 224 383 240, e-mail: dvorakovas@tf.czu.cz